Final Report Under Contract No. NAS 8-28297

for support of

The Study and Development of an Active Scattering Particle Size Spectrometer for Space Environments

prepared for

George C. Marshall Space Flight Center, NASA, Huntsville, Alabama

by

Dr. Robert G. Knollenberg

Particle Measuring Systems
5469 Western Ave.
Boulder, Colorado 80301

December 20, 1972

This final report is divided into three separate parts. The first part is a summary of work accomplished during the performance of the contract. The second part is a report on the " Feasibility Study of Laser Operations in a Vacuum ". The final part is a review of some work in progress at PMS relating to the "Theoretical Response of Active Scattering Particle Spectrometers". The three parts are arranged such that they can be removed - out of context - and stand alone.

PART I

SUMMARY OF WORK ACCOMPLISHED

PART I

Summary of Work Accomplished

The work under this contract was initiated during June, 1972 with early work concentrating on the study of laser operation in a vacuum. Part II details this study which resulted in a laser design which allowed the laser plasma tube and electrodes to be sealed off from the vacuum. Thus the whole question of potential electrical and thermal problems relating to laser operation in a vacuum was precluded. The majority of the work conducted under this contract was completed on or ahead of schedule with delivery a month ahead of schedule.

The observation of the ASPS in operation brought with it a couple of interesting findings. It was observed that for small particles the scattering signal pulses had some high frequency ripple content. The ripple is believed to arise from two sources. One is the Doppler frequency created by interference of the forward and backward scattered light which can occur when the particle has an axial velocity component. For an axial velocity component of one centimeter per second the Doppled velocity would be in the tens of kHz range. Frequencies were generally observed in the range of 10-100 kHz. However, on occasion frequencies were also observed in this range when particles were essentially stationary. This may be due to mode switching but we are not at all clear at this time how this should arise. Mode switching could not be observed in the output beam intensity distribution nor did the reference beam have within an order of magnitude the percentage of modulation that the scattering pulses possessed.

The scattering pulses often appeared to have 20% modulation. The fact that this ripple frequency is considerably greater than the frequency content of the fundamental pulse frequency would allow for it to be separated by filtering. A correlation study could be performed to determine if the frequency or its percentage of modulation were in any way a function of particle size. The Doppler effect can be estimated and controlled by varying particle trajectories. We believe these observations demand closer scrutiny and study. PMS will perform such studies in the future on internal funds if outside support cannot be found to further this work.

The calibration of the two ASPS size ranges involved both theoretical and emperical studies. The two system's theoretical calibration curves of scattering signal versus size closely match an r^2 function. The only discrepancy being in the range of 0.1 to 0.3 microns where the curve is valid only for high refractive indices. This is not believed problematic in that low refractive index materials would be rare in a hard vacuum since these are the more volatile species. Thus, no attempt was made to fit the pulse height detector response to other than an r^2 function. This also gives interchangeability between the pulse height detector circuit boards which is the fastest procedure when trouble shooting.

PART II

FEASIBILITY STUDY OF LASER OPERATIONS IN A VACUUM

I. INTRODUCTION

II. THE HEAT DISSIPATED BY LASER PLASMA TUBES

III. THE EFFECT OF ATMOSPHERIC PRESSURE ON OPEN CAVITY LASER OPERATION

IV. EFFECTS OF LASER HIGH VOLTAGES IN A VACUUM

PART II

Feasibility Study of Laser Operations in a Vacuum

I. INTRODUCTION

Prior to the design of the ASPS, a study was necessary to determine the operational characteristics of open cavity gas lasers under vacuum conditions. Three questions immediately arise when considering gas laser operation under vacuum conditions. First, the laser dissipates a considerable amount of heat which must somehow be dissipated. Second, a gas laser is an active interferometer which in the design of such for particle size measurements has an extended open cavity. The effect of the change in medium--from one atmosphere air pressure to a hard vacuum must be considered as having possible effects on laser cavity stability. Thirdly, the high potentials necessary to start and sustain laser action require protection to avoid electrical discharges and corona. Other questions could also be considered, such as particle trajectories at velocities under vacuum conditions. However, these are obviously factors which could not be resolved nor influence laser operating characteristics.

What follows are three separate sections which largely deal with theoretical considerations connected with the thermal, interferometric and electrical problems, or otherwise influences of laser operations under vacuum conditions. The fourth section extracts basic design criteria from the previous three sections and summarizes the thoughts behind PMS's decision to seal off the laser plasma envelope and its electrodes from the vacuum.

II. THE HEAT DISSIPATED BY LASER PLASMA TUBES

Laser plasma tubes of the type used in ASPS systems generally use a gas fill mixture which generates about 150 volts/in drop along the discharge path length. With an 8" long plasma tube, a voltage drop of 1200 volts would be anticipated. A current of 4ma would thus generate a power dissipation of about 5 watts.

The Ballast resister is normally placed at the anode of lasers and its power dissipation would also cantribute to the total (approximately I^2R= ($.004^2$ x 125K = 2 watts). However, we have operated ASPS lasers with ballast separations of several feet without difficulty and always contained such ballast within the power supply.

The 5 watts may be radiated in whole, or in part, or conducted away by a mounting structure. The two extremes to consider for the radiative problem were for the laser envelope to be looking at infinity with an effective radiative equalibrium temperature of 0° Kelvin or infinity with an effective radiative equalibrium temperature of 300° K. The computed radiative equilibrium temperatures of the laser plasma tube for these two extremes are 376°K and 414°K respectively[1]. From this it is obvious that the laser would require some conduction to keep the temperature below the softening point of the epoxy used to seal the mirrors and Brewster's windows. PMS found that an aluminum mount having contact with 60% of the plasma envelope and a conducting cross section of 3 cm^2 would be required to keep the envelope within 10°C of ambient (metal to which tube mount connects is here considered to be at

---

[1]An emissivity of 0.96 was used for glass envelope of 42 cm surface area.

ambient temperature. It is obvious from the above analysis that the thermal problem created by laser operation in a vacuum is an important consideration for ASPS system design.

III. THE EFFECT OF ATMOSPHERIC PRESSURE ON OPEN CAVITY LASER OPERATION.

In the analyses of the effects of pressure variations one must consider two different cavity geometries. The plasma tube best suited for ASPS measurements is a hybrid tube with one sealed mirror. The mirror configuration is hemispherical (one plane mirror and one spherical mirror) which gives a conical shaped energy density distribution for the laser beam as depicted in Figure 1. As shown, this configuration is most often used to size submicron particles. The mirrors are reversed for measurements of large particles. Thus, the open cavity region is bounded by a Brewster's window and either a plane or spherical mirror. Since the radius of curvature of the curved mirror is extremely large compared to the size of the beam, the geometry of the beam is nearly a perfect wedge with either plane or spherical mirror (see Figure 2). This wedge has a refractive index of 1.0002922 for air or 1.000 for a perfect vacuum. It has the effect of displacing the beam on amount which can be calculated. The degree of misalignment that can be tollerated varies with the mode tuned. For TEM_{00} operation Bloom (1968)[1] gives a value of 5 minutes as to the angular allowance tollerable. For higher order modes, the margin increases approximately linearly with the degree of ordering. In our case, we must consider the fact that it is necessary to tune the laser at ambient air pressure prior to vacuum introduction. Thus, one is interested in the change in power output and the amount of mode shifting.

The computed angular error due to a change of medium pressure from one atmosphere to a perfect vacuum is only 16 seconds. Thus, the only potential problem might conceivably be mode shifting. To examine the possible effects

---

[1]Bloom, Arnold: 1968, Gas Lasers.

ACTIVE SCATTERING AEROSOL SPECTROMETER
OPTICAL SYSTEM FOR 0.1 TO 1.5 μ AEROSOL SIZE RANGE

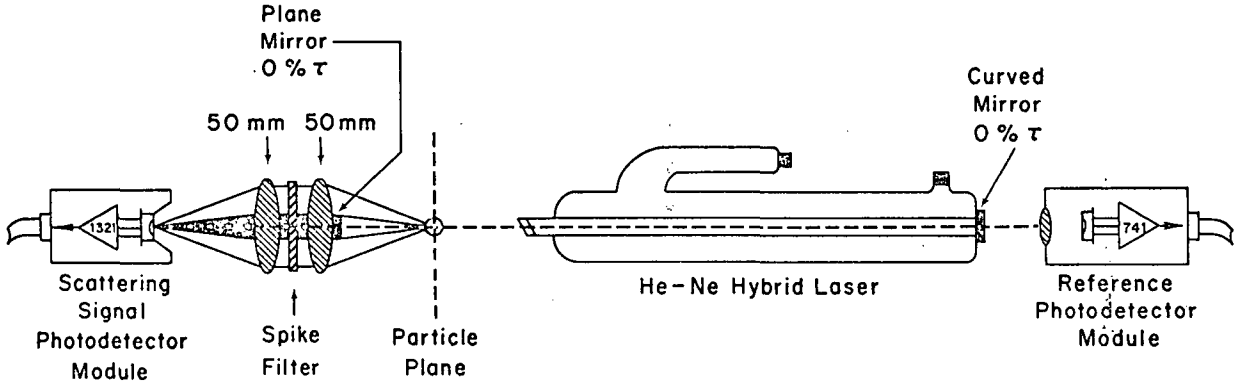

NOTE: MIRRORS REVERSED FOR 1-25 μ RANGE

FIGURE 1. Optical System Diagram for ASPS Systems

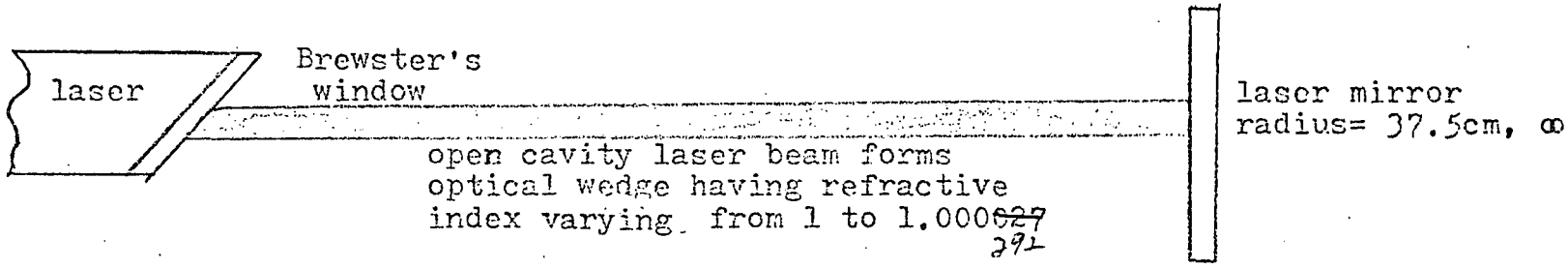
laser
Brewster's window
laser mirror
radius= 37.5cm, ∞
open cavity laser beam forms optical wedge having refractive index varying from 1 to 1.000292

FIGURE 2

of mode shifting experiments were conducted at PMS to determine the amount of angular detuning necessary to produce mode shifting. A precision mirror gimble was used where differential micrometers could read displacements to 10". The measured error required to shift from TEM_{01*} to TEM_{01} or TEM_{00} was __2__ minutes and __3__ minutes respectively. Thus, no problem would be expected from the effects of air pressure reduction to vacuum.

PMS also analyzed data from vacuum ASPS operations at the Martin Marietta Corporation during an MSFC funded SKYLAB contamination ground test program (SCGTP) during May, 1972. Those results indicated that mode shifting did not occur at pressures reduced from approximately 0.8 atmospheres to 10^{-9} atmospheres.

IV. EFFECTS OF LASER HIGH VOLTAGES IN A VACUUM

The high voltages required for laser ignition and continuous operation demand particular attention. It must first be remarked that the pressure range over which system operation is desired may encounter any of the basic ionization related electrical phenomenon generally classified as spark breakdown, glow discharges (corona), or self-sustaining electrical arcs.

First we will consider the nature of the expected laser operating potentials. Figure 3 shows the voltage-current characteristics of the plasma tubes used in ASPS systems. Two characteristics are particularly worth noting. First, before the operating range can be reached a high voltage must be applied to initiate ionization. Second, in the operating region there is a negative resistance. The negative resistance region of the tube VOLTAGE-AMPERAGE characteristics require a limit to the supply current provided by a ballast resister of 125K ohms to 150K ohms. The power supply block diagram of Figure 4 shows a basic high voltage supply (1600V) with an add-on higher voltage doubler which has an added trippler network in series (High voltage ionizer network) prior to ignition and subsequent effective shorting through the ballast resister.

Prior to laser ignition, the anode voltage nears 2500 V and this becomes the highest potential for consideration. However, it should be pointed out that electrical discharges often require a certain "charging" time at the discharge potential prior to the actual discharge. This may be longer than the time required for laser ignition and thus preclude the external discharge. Thus, the actual ignition time is of some significance. To isolate the various aspects of the problem, we considered the three types of ionization phenomenon separately beginning with spark breakdown.

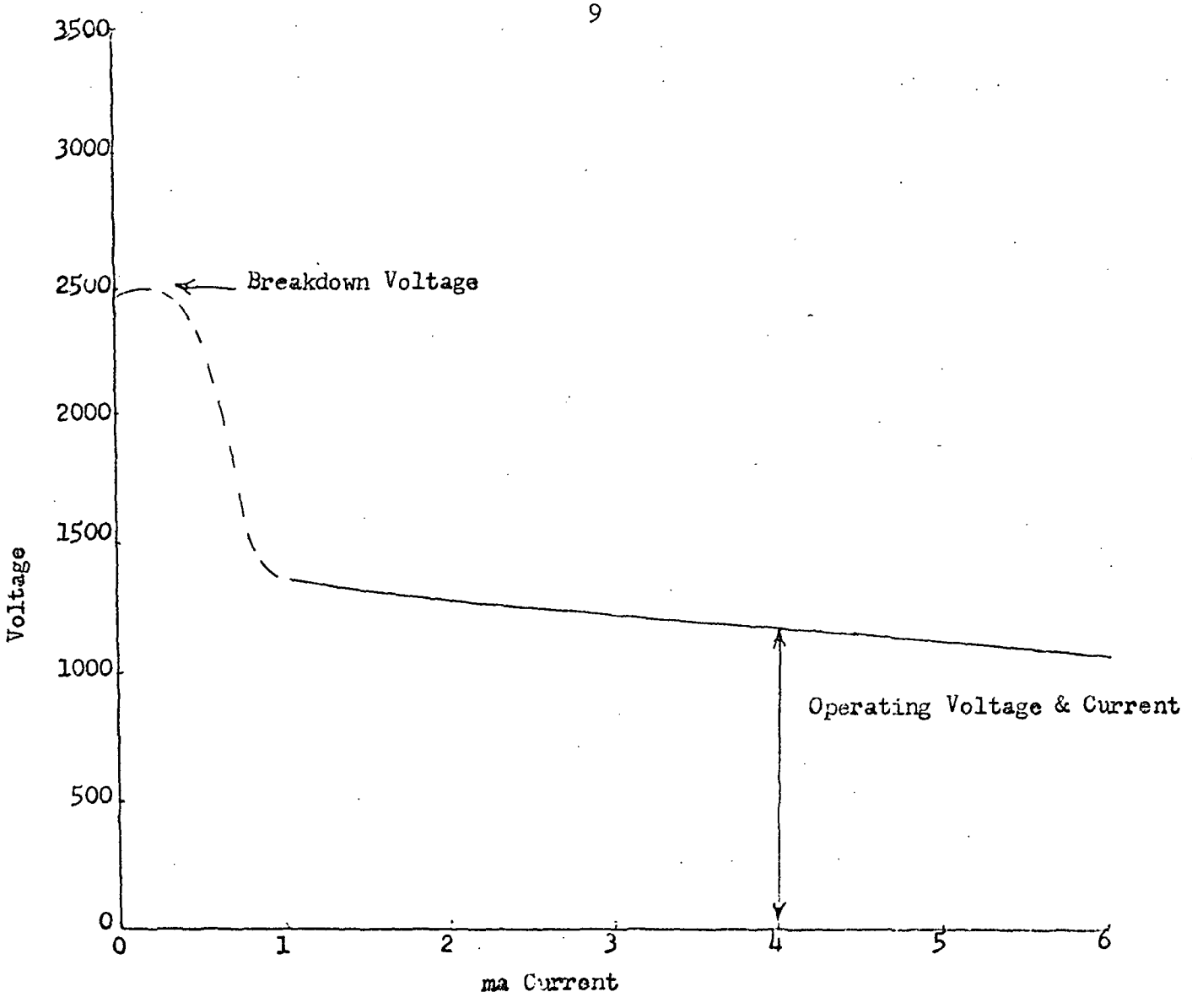

Figure 3. Current-Voltage Characteristics of ASPS Lasers

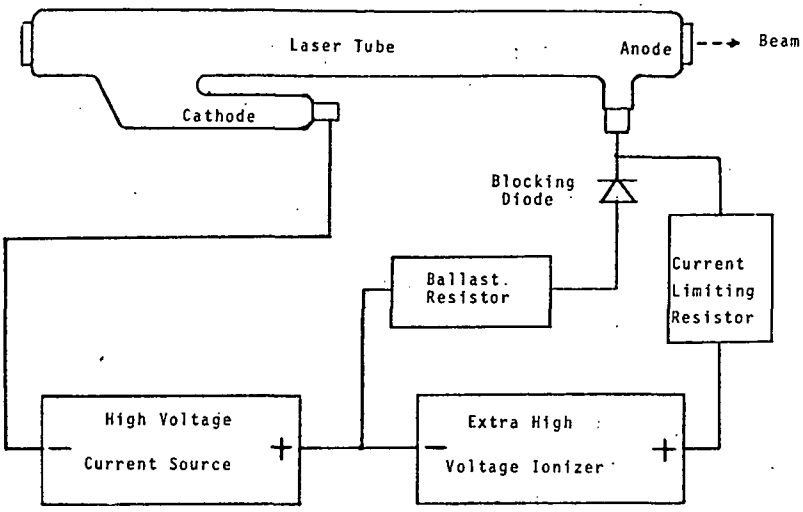

LASER POWER SUPPLY BLOCK DIAGRAM

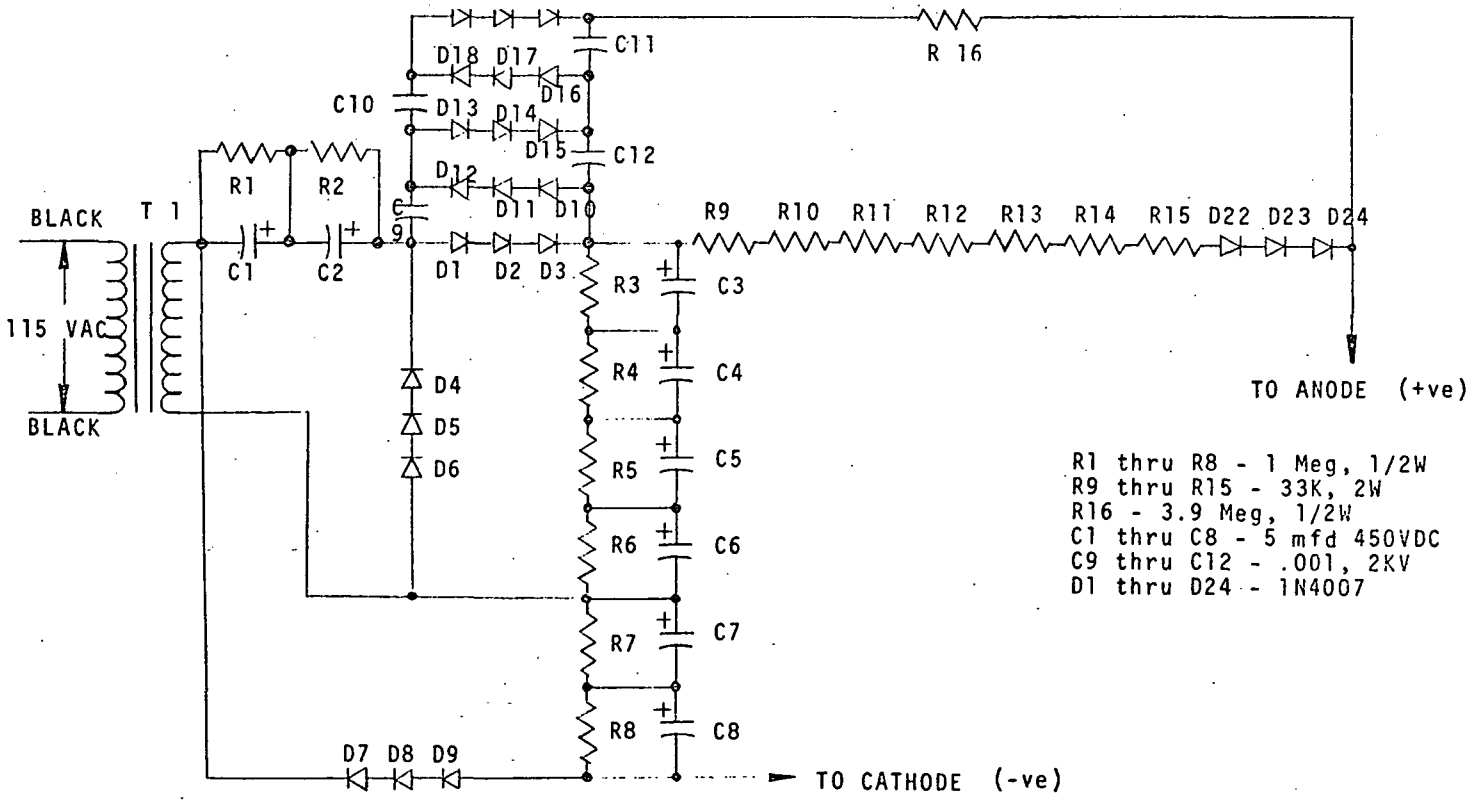

LASER POWER SUPPLY CIRCUIT DIAGRAM FOR 1600 V.

FIGURE 4

As the electrical field between the anode of the laser and some external point (e.g., nearest ground potential such as cathode or a mounting structure which is near ground potential) increases, the current increases steadily until some point there is a sudden transition from the TOWNSEND, or "dark" discharge to one of several forms of self sustaining discharge. This transition or spark consists of a sudden change in current across the gap. For plane parallel electrodes, the result is a spark that can initiate an arc discharge. For sharply curved electrodes, there may be corona or brush discharge. These latter discharges will be considered later. Under some conditions the change in current may be quite small and the examples are typical but not singular in definition. For example, when a corona discharge occurs between a cylinder and coaxial wire this initial corona discharge, although a self sustaining discharge, represents an incomplete failure of the gap occuring only in a limited region near electrodes of small radius of curvature, while the rest of the "gap" carries a "dark" current. In an engineering sense, breakdown is generally considered to occur only when the entire "gap" is bridged with the establishment of an arc discharge as common.

1. Sparking-Potential.

It was experimentally determined by PASHEN in 1889 that the sparking potential is a function of the product of the density and gap length only. However, most workers use the product of pressure and gap length. The sparking potential for air at one atm. pressure is given by

$$V_S = 30d + 1.35 \text{ (kV)}.$$

the spark-breakdown voltage has a minimum value at a critical value of pressure and distance (d) as shown in Figure 5. The important information here is the minimum sparking potential of about 325 Volts for a separation of 1mm

FIGURE 5 PASCHEN CURVE FOR AIR

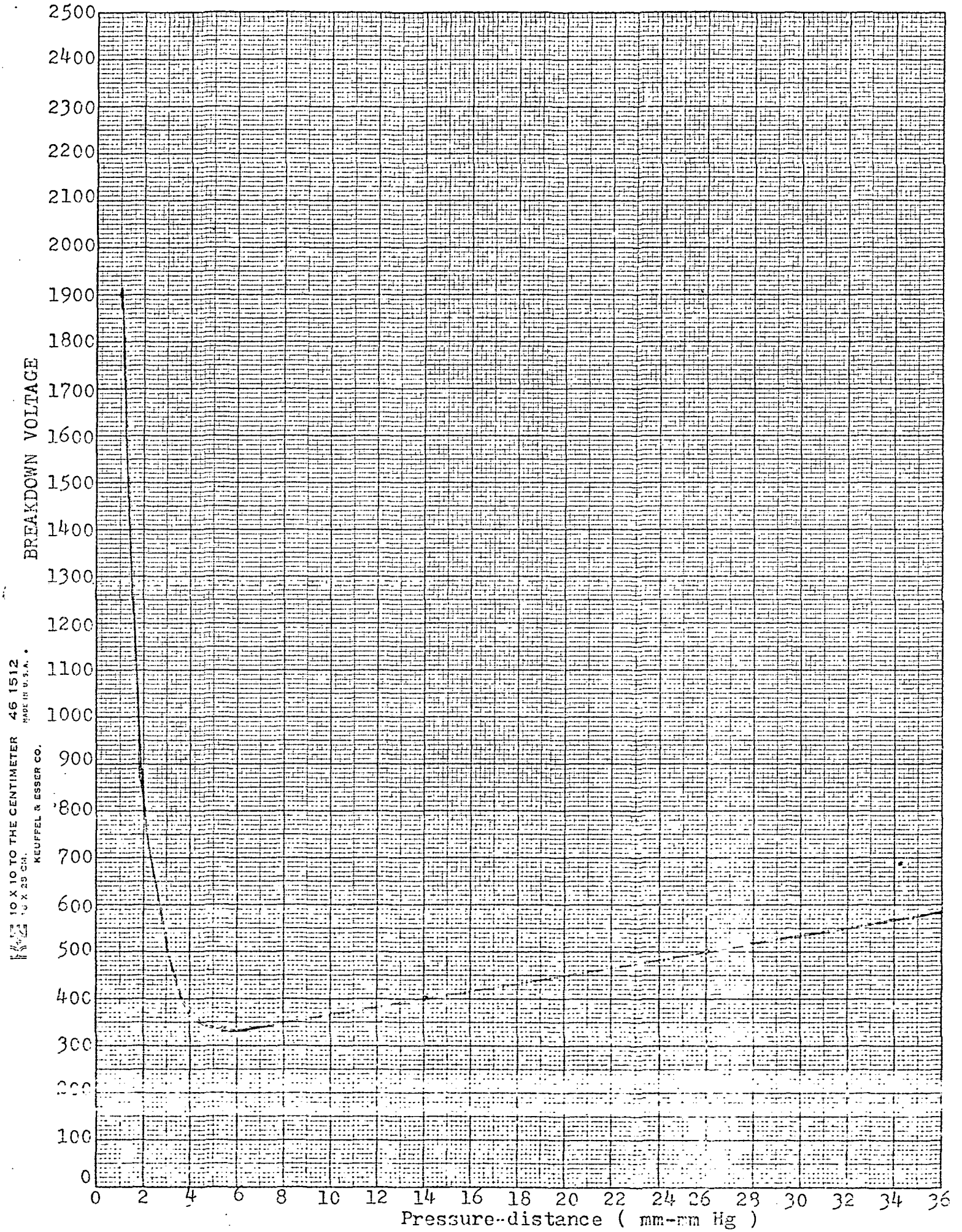

and pressure of 5.5 torr, or $^1/_2$ torr and 1 cm. Since the likely separation is of the order of a centimeter or two, the greatest potential problem is likely to occur at a pressure between 10^{-1} and 1 torr.

2. Corona Discharge.

The electric field strength (critical corona gradient) at which corona discharge begins is nearly the same as for spark discharge. In spite of the uncertainties involved in the derivation of the required field strengths for corona discharge, they compare most favorably with the emperical relationships given by PEEK (1925). Corona is distinguished by the fact that increasing the separation between sharply curved surfaces, such as corners and points, generally results in the breakdown of the gas near the surfaces less than the spark-breakdown voltage. This breakdown appears as a glow discharge. While weak corona may not prohibit laser operation its persistance causes a deterioration of insulating materials. Corona from an anode was generally characterized by bluish coloration over the entire anode while corona at the cathode (required grounding of the anode since the cathode normally runs within a hundred volts of ground) was characterized by red filaments of glowing gas along points and edges of the cathode. The critical corona gradient depends only on the radius of the anode (or surface features of the anode) and is not markedly affected by the effective "gap" distance. This independence of spacing is expected since for large separations the field at the surface of the anode would be relatively unaffected by further separation. This fact, that the critical field strength depends only on the anode radius facilitates the estimation of the minimum radius of curvature of metal parts used at high voltages. In the case of the ASPS lasers, the anode radius is 4 mm. The critical corona gradient is given for parallel wires by PEEK as

$$E_c = 30 m b \left(1 + \frac{0.301}{8a}\right) \text{ (max. kV/cm)}$$

where b is the pressure in torr and T is the temperature in degrees Kelvin.

It should also be remarked that the mechanisms of discharge about the anode is quite unlike that for the cathode. In the case of the cathode positive ions are formed and accelerate in the cathode field to produce the necessary electrons for a self-sustaining discharge. In the case of the anode, electrons formed in the surrounding space by various ionizing radiations always present accelerate in the direction of the anode establishing electron avalanches. These avalanches maintain the ionized state near the anode.

3. Arc Discharge.

The electric arc is a self sustaining voltage having a low voltage drop and capable of supporting high currents. This is the type of discharge already discussed with regard to laser operation. At atmospheric pressures the arc is characterized by a small brilliant core surrounded by a cooler region of flaming gases (Aureole) which is a region of chemical activity. Because of the high temperatures of the core, the gases are largely dissociated. At low pressures, the appearance of the arc depends upon the slope of the discharge tube. A constricted tube such as a laser capillary thus gives a bright glow even at low pressures. The absence of such a confining structure around the laser envelope makes it unlikely that arcing would occur external to the laser at low pressures. At higher pressures, the laser power supply simply cannot deliver the required current. Thus arcing was not considered in the establishment of the design criteria for laser operation in a vacuum.

4. Summary of Design criteria and Final Design.

The preceeding sections developed and discussed the theory relevent to potential problems with laser operations in the pressure range

from one atmosphere to a hard vacuum. The choices available to PMS for operating the laser were two: (1) operate the plasma tube in the vacuum and provide adequate sealed insulation around the laser electrodes to prohibit spark-discharge and corona, or (2) devise a seal for the laser plasma tube which would allow the laser electrodes to operate at ambient pressure. From tests it was determined that to operate the laser tube in the vacuum the electrodes would have to be potted in an epoxy or silastic material. (the minimum value in the Pashen curve of 325 Volts would provide for only 1 cm separation at pressures of 0.1 to 1 torr). Thus, one would estimate that a separation of centimeters would be required if the laser electrodes were not sealed over completely. A second point for consideration is the necessity to dissipate the heat as discussed in section 2. The amount of metal required to conduct away the heat places difficulty on establishing its safe separation from the electrodes. Thus, the sealed insulation of laser electrodes is again required so that this separation distance can be reduced without increasing electrical problems.

One final factor that detracts from potted electrodes is the necessity to cable power from the power supply (at ambient pressure) to the laser (in vacuum). A connector vacuum penetration is required. If this connector is not totally sealed, its pins produce another potential spark-discharge or corona problem[1]. Such a connector if sealed would lose utility and re-potting work would be necessary every time the laser had to be removed or replaced.

In summary, the laser plasma tube was found to present a considerable problem if one was to insure its safe operation under vacuum conditions. On

---

[1]Testing by PMS conclusively showed that Corona would develop between connector pins where laser voltages were applied.

the other hand, the change of medium from one atmosphere air pressure to a hard vacuum within the open cavity laser section would present no descernable change in laser operating characteristics. Thus, the logical conclusion to be followed was to devise a seal for the laser plasma tube which would allow the electrodes and bulk of the plasma tube to operate at ambient air pressure. Such a seal was designed and tested at PMS.

For the seal to be safe, it was necessary to have special laser plasma tubes designed which had the cathode placed nearest the Brewster's window and with ample space between the cathode side-arm and the Brewster's window to epoxy the laser envelope into a stainless steel mount. This stainless steel mount was constructed with a VITON "O" ring seal which is compressed using 4 socket head screws. The epoxy can be most any commercial clear apoxy having a long curing time. This long curing time allows for complete out-gasing and the best laser to metal seal. It is the opinion of PMS that this seal is superior to the standard seals used in the construction of the laser itself and thus is not expected as a point of failure.

PART III

THEORETICAL RESPONSE OF ACTIVE SCATTERING PARTICLE SPECTROMETERS

PART III

Theoretical Response of Active Scattering Particle Spectrometers

The scattering of electromagnetic radiation within an open cavity laser was recently modeled by R. G. Knollenberg at PMS. A computer program was devised to compute the scattered energy for spheres having variable radii and refractive indices in a plane wave. It was recognized that in the ASPS the collected light signal consists of both forward and backward scattered light and that these can constructively or destructively interfere. However, after further analysis it was recognized that the only time the backward scattered light accounts for even 10% of the total light signal is when the particle size is considerably less than the wavelength and under such conditions the phase difference between the forward and backward scattered light is nearly the same. Thus, the MIE scattering computations are adequate in their classical form and the necessity to solve the problem of electromagnetic scattering in a standing wave was precluded.[1]

The computation involves only four input parameters; wavelength (λ) radius (r), refractive index (m) and scattering angle (θ). The particle radius and wavelength are generally combined into an parameter x given by:

$$x = 2 \pi r/\lambda$$

Because of the large variation in scattered energy (intensity) with angle, a logorithmic plot is used. A sample of such a calculation is shown in Figure 1 for a particle radius of 1.0 micron and a refractive index of 1.6 (Real) with no absorbtion (imaginary part of refractive index = 0.

---

[1]To this writer's knowledge, the problem of electromagnitic scattering in a standing wave has not been solved theoretically in exact form. The boundary conditions would appear not identical to those given by MIE.

Computer Plotted Intensity vs Scattering Angle for a 1.0u Radius Sphere having a Refractive Index = 1.6 at 6328A°. Solid line is total intensity. Dashed and dotted lines are the components for the two polarizations.

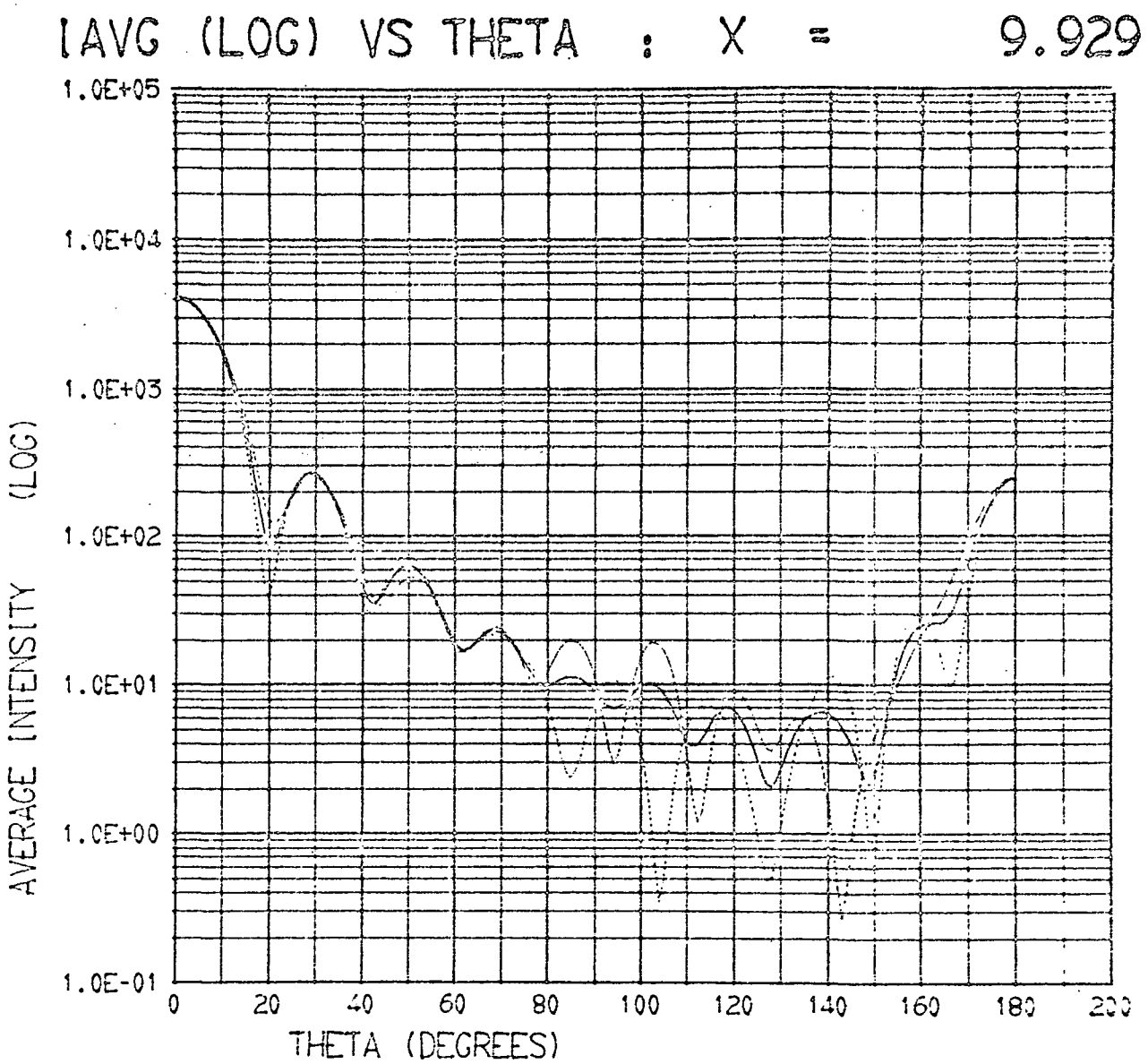

FIGURE 1

In addition to this computation, the total scattered power was integrated for each degree step to enable the determination of the amount of scattered energy received by the collecting optics in ASPS systems. Printouts of these incremental scattered intensities are shown in Figure 2 for scattering angles of 1-28 degrees and 152 to 180 degrees. The quantity ITSUM is the total scattered energy collected over 4π steradians. It serves as a normalization parameter and can be used to estimate the efficiency of the collecting optics.

Note the uniformity of scattering signal vs. angle over collecting angles up to 20°. The sum over the collecting aperture of 5-20° assures a smooth calibration for ASPS instruments at least in the vicinity of one micron as shown here (see figures 3a & 3b). At radii of 0.1 and less, the refractive index can cause a change in scattering power by nearly 4. Choosing a refractive index value of 1.6 allows for an uncertainty of ±2 in scattered intensity for completely unknown refractive index. This results in an error of ± v 2 in terms of particle radius which would account for much less than the specified rms error of ±0.1 microns. If the refractive index of sized particles is known, one should use the theoretical computation for that refractive index for the most exact results.

We have run computations for real refractive indices from 1.3 to 2.5 at intervals of 0.1. The computations are made every 0.1° and for radius intervals of 0.1 micron for radii up to 100 microns. The resulting computations are filed on 90,000 frames of microfilm at PMS and are available from PMS. The entire program is listed on the following pages. This program requires a considerable amount of machine time and certain plotting routines are not generally available at most institutional computation centers. Questions regarding its use should be directed to R. G. Knollenberg.

Computer Printout of Energy Scattered into Incremental Solid Angles. Note: ITSUM = The total scattered energy collected over 4II steradians.

ITSUM= 7.228226E+02

X = 9.929

1	3.974489E+00	152	2.140785E-01
2	1.175245E+01	153	2.969521E-01
3	1.893026E+01	154	4.017424E-01
4	2.525645E+01	155	5.204576E-01
5	3.057897E+01	156	6.424161E-01
6	3.416220E+01	157	7.557781E-01
7	3.647802E+01	158	8.490800E-01
8	3.731013E+01	159	9.132155E-01
9	3.673160E+01	160	9.431250E-01
10	3.489594E+01	161	9.390176E-01
11	3.202285E+01	162	9.068911E-01
12	2.857984E+01	163	8.577751E-01
13	2.426149E+01	164	8.069545E-01
14	1.996791E+01	165	7.710774E-01
15	1.578425E+01	166	7.659558E-01
16	1.196256E+01	167	8.034859E-01
17	8.707275E+00	168	8.892970E-01
18	6.165058E+00	169	1.021008E+00
19	4.419454E+00	170	1.187634E+00
20	3.490543E+00	171	1.370262E+00
21	3.337842E+00	172	1.543998E+00
22	3.870398E+00	173	1.680966E+00
23	4.954145E+00	174	1.755977E+00
24	6.428276E+00	175	1.740347E+00
25	8.116868E+00	176	1.625521E+00
26	9.843514E+00	177	1.434659E+00
27	1.144347E+01	178	1.185520E+00
28	1.277675E+01	179	6.860941E-01
		180	2.347514E-01

FIGURE 2

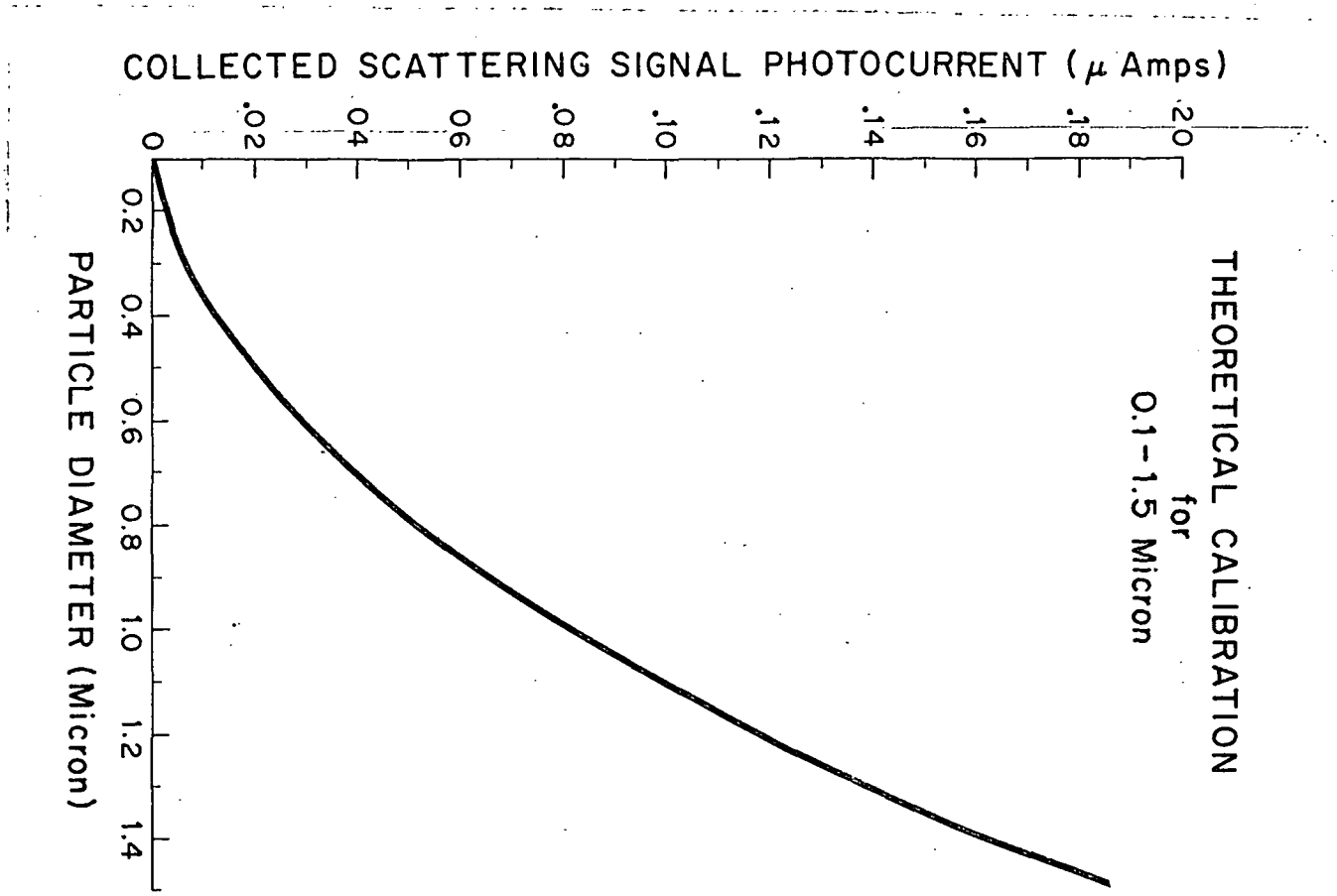

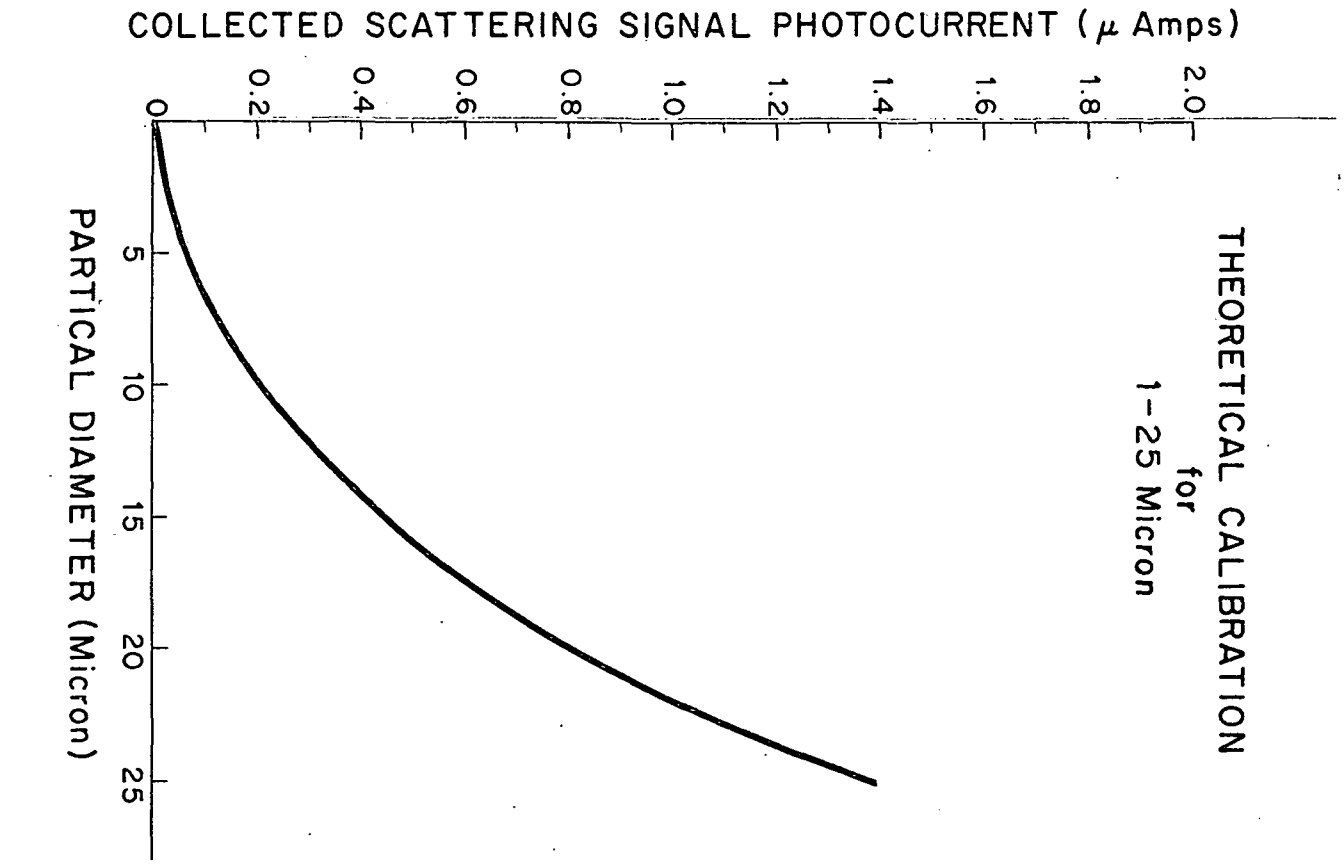

Figures 3A and 3B. Calibration Curves for MSFC ASPS System

Computations as just described were used to calibrate the ASPS size ranges. This theoretical calibration is approximate in that it does not account for particle shapes other than spheres. The selection of the collecting angles minimizes the effects of irregular shaped particles. In the large particle size range, calibrations were performed with polystyrene and glass spheres as well as samples of irregular shaped particles. These all support the theoretically derived calibration curves.

```
JOB,5197,V0120012,KNOLLENBERG
TRAP
LIMIT,DD80=3000
LIMIT,PR=2000
LIMIT,T=60
FORTRAN
      PROGRAM MIEA
C             RRA 42    PARTICLE MEASURING SYSTEMS, BOULDER, COLORADO
C     MIE SCATTERING ANALYSIS                                          2
      COMPLEX W(400),A(400),SA(400),SB(400),SA2(400),SB2(400),S1(181)
     1 ,S2(181),ENT1(181),ENT2(181),PM,WO,WM1,AO,ACONJ,BCONJ,S1CONJ,
     2  S2CONJ,TEMP2C,TEMP3C,TEMP4C,TEMP5C
      DOUBLE THETA(181), DTHETA, CONST1, CONST2
      DIMENSION THET(181),S1RE(181),S1IM(181),S2RE(181),S2IM(181),
     1 ENTAVG(181),PI(400),TAU(400),RSA2(400),RSB2(400),RENT1(181),
     2 RENT2(181),URSA(400),URSB(400)
      DIMENSION LTT(4),LTX(4),LTY(4)
      DIMENSION RSA(400),RSB(400),ENT3(181),ENT4(181),POLAR(181)
      DIMENSION IT(181),CTHTS(181),LIT(4),LITT(4)
      DOUBLE DTHETI
      REAL IT,ITSUM
   40 FORMAT (*-NTHET = * I10, * BUT SHOULD BE .LE. 181*)
   50 FORMAT (2I5)
   55 FORMAT(///,10X,36HTERMINATION CONDITIONS NOT SATISFIED)           015
   65 FORMAT (35X *SIZE PARAMETER = * F10.4, 10X *DTHET = * F5.2 /)
   70 FORMAT (2E10.5, D5.2, I5, F10.5)
   75 FORMAT (18X *INDEX OF REFRACTION     ( REAL PART = * F10.6, * ,
     1  IMAGINARY PART = * E10.6, * )* /)
   85 FORMAT(  3X,16HSCATTERING ANGLE,10X,2HI1,15X,2HI2,15X,2HI3,15X,
     1 2HI4,14X,4HIAVG,9X,12HPOLARIZATION / 9X *THETA* /)
   95 FORMAT(8X,F6.2,5X,  6E17.6)                                       021
  105 FORMAT (46X *SIZE PARAMETER = * F10.4 / )
  115 FORMAT (10X *N* 7X 2(7X *A SUB N*) 3X 2(7X *B SUB N*) 9X *(A SUB N
     1)* 3H**2 6X *(B SUB N)* 3H**2 / 16X 2(10X *REAL* 8X *IMAGINARY*)/)
  125 FORMAT(9X,I3,9X,1H(,  E11.4,3H , ,E11.4,1H),4X,1H(,E11.4,         026
     1 3H , ,  E11.4,1H),7X,  E11.4,7X,  E11.4)
  135 FORMAT (*-* / *-EFFICIENCY FACTOR FOR EXTINCTION = * E12.6)
  145 FORMAT (      *-EFFICIENCY FACTOR FOR SCATTERING = * E12.6)
  155 FORMAT (*-* / *-* / *-* 10X *THIS PROGRAM WAS PROVIDED THROUGH THE
     1 COURTESY OF PARTICLE MEASURING SYSTEMS, BOULDER, COLORADO*)
  165 FORMAT (*1* 35X *A SUB N AND B SUB N COEFFICIENTS OF MIE FUNCTIONS
     1*/)
  175 FORMAT (3X *SCATTERING ANGLE* 7X *AMPLITUDE S SUB 1* 14X *AMPLITUD
     1E S SUB 2* / 9X *THETA* 2X 2(10X *REAL* 8X *IMAGINARY*) /)
  185 FORMAT(8X,F6.2,7X,1H(,  E11.4,3H , ,E11.4,1H),4X,1H(,E11.4,       035
     1 3H , ,  E11.4,1H))
  195 FORMAT (*1* 40X *COMPUTATION OF MIE SCATTERING FUNCTIONS* /)
  205 FORMAT(6E10.2,8X,I4,I4,4H MIE)                                    038
  215 FORMAT(  4E15.6,8X,I4,I4,4H MIE)                                  039
  225 FORMAT(  3E18.6,14X,I4,4X,4H MIE)                                 040
  245 FORMAT (*1* 20X *AMPLITUDE FUNCTIONS FOR MIE SCATTERING* /)
  265 FORMAT ( 1X *INDEX OF REFRACTION     ( REAL PART = * F10.6, * ,
     1  IMAGINARY PART = * F10.6, * )* /)
  275 FORMAT (15X *SIZE PARAMETER = * F10.4, 10X *DTHET = * F5.2 /)
  285 FORMAT (*-* / *-* / *-ELAPSED TIME FOR THIS CASE = * E10.2,
     1  * SECONDS.*)
  310 FORMAT (*-NORMALIZATION FACTOR = * E12.6)
  315 FORMAT (*1*)
```

```
C                                                                       47
      DATA (TEST2 = 1.0E-14)
C
C
      WRITE(6,155)
      READ(5,500) LTT,LTX,LTY,LIT,LITT
  500 FORMAT(4A10)
      CONST1 = 3.14159265358979323846264300
      CONST2 = CONST1/180.0D0
      DTHETI=0.
      XLAM=.6328E-6
      READ(5,70) PM,DTHETA,NTHET,RX
  100 TIMEIN = TIMEF(0)
      ITSUM=0
      RX=RX+0.1E-6
      IF(RX.EQ.0100.E-6) GO TO 1002
      X=2*CONST1*RX/XLAM
      ENCODE(10,501,LTT(4)) X
      ENCODE(10,501,LITT(4)) X
  501 FORMAT(F10.3)
      WRITE(6,203)X
  203 FORMAT(///,50X,'X = ',F10.3)
      DTHET = DTHETA
      IF (NTHET) 103,1000
  103 IF (NTHET .GT. 181) GO TO 1001
      R=REAL(PM)                                                        *58
      RP=AIMAG(PM)
      TEMPRP = RP                                                       59
      RP=-RP
      OTH=1.2*X+9.0
      SN=SIN(X)                                                         71
      CN=COS(X)                                                         72
      POWP=RP*X                                                         73
      POW=R*X                                                           74
      TEMP1 = EXP(POWP)
      TEMP2 = 1.0/TEMP1
      HSIN = (TEMP1 - TEMP2)/2.
      HCOS = (TEMP1 + TEMP2)/2.
      WO=CMPLX(SN,CN)                                                   078
      WM1=CMPLX(CN,-SN)                                                 079
      TEMP1 = SIN(POW)
      TEMP2 = COS(POW)
      TEMP3 = TEMP1**2 + HSIN**2
      AREAL = TEMP1*TEMP2/TEMP3
      AIMA = HSIN*HCOS/TEMP3
      AO=CMPLX(AREAL,AIMA)                                              082
      TEMP1 = 1.0/X
      W(1) = TEMP1*WO-WM1
      W(2) = 3.0*TEMP1*W(1)-WO
      TEMP2C = TEMP1/PM
      A(1) = -TEMP2C + 1.0/(TEMP2C - AO)
      WREAL=REAL(W(1))                                                  086
      WREALO=REAL(WO)                                                   087
      TEMP3C = A(1)/PM + TEMP1
      TEMP4C = A(1)*PM + TEMP1
      SA(1) = (TEMP3C*WREAL - WREALO)/(TEMP3C*W(1) - WO)
      SB(1) = (TEMP4C*WREAL - WREALO)/(TEMP4C*W(1) - WO)
C                                                                       91
```

```
      DO 102 N=1,400
      N1=N+1
      N2=N+2
      PN=N
      PN1=N1
      TEMP2 = (2*N2-1)*TEMP1
      W(N2) = TEMP2*W(N1) - W(N)
      WREAL=REAL(W(N1))
      WREAL1=REAL(W(N))
      TEMP3C = PN1*TEMP2C
      A(N1) = -TEMP3C + 1.0/(TEMP3C - A(N))
      TEMP3 = PN1*TEMP1
      TEMP4C = A(N1)/PM + TEMP3
      TEMP5C = A(N1)*PM + TEMP3
      SA(N1) = (TEMP4C*WREAL - WREAL1)/(TEMP4C*W(N1) -W(N))
      SB(N1) = (TEMP5C*WREAL - WREAL1)/(TEMP5C*W(N1) -W(N))
      RSA(N)=REAL(SA(N))
      RSB(N)=REAL(SB(N))
      URSA(N)=AIMAG(SA(N))
      URSB(N)=AIMAG(SB(N))
      ACONJ=CONJG(SA(N))
      BCONJ=CONJG(SB(N))
      SA2(N)=SA(N)*ACONJ
      SB2(N)=SB(N)*BCONJ
      RSA2(N)=REAL(SA2(N))
      RSB2(N)=REAL(SB2(N))
      TEST1=(RSA2(N)+RSB2(N))/PN
      IF(TEST1-TEST2)3,2,2
    2 IF(PN-OTH)102,3,3
  102 CONTINUE
      WRITE(6,55)
    3 KEEPN=N
C
   99 DO 5 I = 1,NTHET
      THETA(I) = FLOATF(I-1)*DTHETA  + DTHETI
      THET(I) = THETA(I)
      IF(THET(I).LE.180.) GO TO 7
      NTHET=I-1
      GO TO 6
    7 CTHETA = SNGL(DCOS(THETA(I)*CONST2))
      CTHTS(I)=CTHETA
      STHETA = SNGL(DSIN(THETA(I)*CONST2))
      S1(I)=CMPLX(0.,0.)
      S2(I)=CMPLX(0.,0.)
      PI(1)=1.
      PI(2)=3.0*CTHETA
      TAU(1)=CTHETA
      TEMP4 = STHETA**2
      TAU(2) = 3.0*(CTHETA**2 - TEMP4)
C
      DO 4 N=1,KEEPN
      N1=N+1
      N2=N+2
      TEMP2 = 2*N2-1
      TEMP3 = N2-1
      PI(N2) = (TEMP2*PI(N1)*CTHETA - N2*PI(N))/TEMP3
      TAU(N2) = CTHETA*(PI(N2)-PI(N)) - TEMP2*TEMP4*PI(N1) + TAU(N)
      TEMP2 = 2*N+1
```

```
      TEMP3 = N*N1
      TEMP2 = TEMP2/TEMP3
      S1(I) = TEMP2*(SA(N)*PI(N)+SB(N)*TAU(N))+S1(I)
      S2(I) = TEMP2*(SB(N)*PI(N)+SA(N)*TAU(N))+S2(I)                    145
    4 CONTINUE
    5 CONTINUE
C
    6 DO 12 I = 1,NTHET
      S1RE(I)=REAL(S1(I))                                               190
      S1IM(I)=AIMAG(S1(I))                                              191
      S2RE(I)=REAL(S2(I))                                               192
      S2IM(I)=AIMAG(S2(I))
   12 CONTINUE
      EXKROS = SCKROS = 0.
      COEPH = 2.0*TEMP1**2
C
      DO 8 N=1,KEEPN
      TEMP2 = (2*N+1)*COEPH
      EXKROS = TEMP2*(RSA(N) + RSB(N)) + EXKROS
      SCKROS = TEMP2*(RSA2(N) + RSB2(N)) + SCKROS
    8 CONTINUE
      ANORM = 4./(SCKROS*X**2)
C
      DO 9 I = 1,NTHET
      S1CONJ=CONJG(S1(I))                                               164
      ENT1(I)=S1(I)*S1CONJ                                              165
      S2CONJ=CONJG(S2(I))                                               166
      ENT2(I)=S2(I)*S2CONJ                                              167
      RENT1(I)=REAL(ENT1(I))                                            168
      RENT2(I)=REAL(ENT2(I))                                            169
      ENT3(I)=REAL(S1(I)*S2CONJ)                                        170
      ENT4(I)=-AIMAG(S1(I)*S2CONJ)                                      171
      TEMP2 = RENT1(I) + RENT2(I)
      POLAR(I) = (RENT1(I) - RENT2(I))/TEMP2
      ENTAVG(I) = TEMP2/2.0
      IF(I.EQ.1) GO TO 9
      IT(I-1)=(ENTAVG(I)+ENTAVG(I-1))*CONST1*(CTHTS(I-1)-CTHTS(I))
      IF(IT(I-1).LE.1.E-12) IT(I-1)=1.E-10
      IBIS=I-1
      WRITE(6,202)IBIS,IT(I-1)
  202 FORMAT(1H0,I4,E15.6)
      ITSUM=ITSUM+IT(I-1)
    9 CONTINUE
      ENCODE(20,5000,IT(3)) ITSUM
 5000 FORMAT(*ISUM=*E15.2)
      TIMEOT = TIMEF(0)
      DELTIM = (TIMEOT - TIMEIN) / 1000.0
      GO TO 9999
C
C     NO. 1 OUTPUT
C
      WRITE(6,165)
      WRITE(6,75) R,TEMPRP
      WRITE(6,105)X                                                     20
      WRITE(6,115)                                                      21
      WRITE(6,125)(N,RSA(N),URSA(N),RSB(N),URSB(N),RSA2(N),RSB2(N), N =
     1 1,KEEPN)
C
```

```
C       NO. II OUTPUT
C
        WRITE(6,245)
        WRITE(6,265) R,TEMPRP                                          217
        WRITE(6,275) X, DTHET
        WRITE(6,175)                                                   220
        WRITE(6,185)(THET(I),S1RE(I),S1IM(I),S2RE(I),S2IM(I), I = 1,NTHET)
C
C       NO. III OUTPUT
C
        WRITE(6,195)
        WRITE(6,75) R,TEMPRP
        WRITE(6,65) X,DTHET
        WRITE(6,85)                                                    187
        WRITE(6,95)(THET(I),RENT1(I),RENT2(I),ENT3(I),ENT4(I),ENTAVG(I),
       1 POLAR(I), I = 1,NTHET)
 9999 CONTINUE
        CALL IDIOT(THET,ENTAVG,NTHET,2,1777B,LTX,LTY,LTT,-1)
        CALL DASHLN(1430B)
        CALL CURVE(THET,RENT1,NTHET)
        CALL DASHLN(1634B)
        CALL CURVE(THET,RENT2,NTHET)
        NTHET1=NTHET-1
        CALL IDIOT(THET,IT,NTHET1,2,1777B,LTX,LIT,LITT,-1)
        DTHETI=THETA(NTHET)
        IF(THET(NTHET).LT.180.) GO TO 99
        WRITE(6,5011) ITSUM
 5011 FORMAT(*0   ITSUM= *E15.6)
      NTHET=181$ DTHETI=0.
        GO TO 100
        WRITE(6,135) EXKROS                                            197
        WRITE(6,145)SCKROS                                             198
        WRITE (6, 310) ANORM
        WRITE (6, 285) DELTIM
        GO TO 100
C
C       END OF RUN
C
 1000 WRITE(6,315)
        GO TO 1002
 1001 WRITE (6, 40) NTHET
 1002 CONTINUE
 1010 CALL FRAME
        CALL EXIT
        END                                                            232
        SUBROUTINE IDIOT(FLDX,FLDY,N,LTYPE,IPATRN,LABX,LABY,LTIT,LFRAME)
C       SUBROUTINE IDIOT(FLDX,FLDY,N,LTYPE,IPATRN,LABX,LABY,LTIT,LFRAME,M)
C       SUBROUTINE IDIOT(FLDX,FLDY,L,LTYPE,IPATRN,LABX,LABY,LTIT,LFRAME,N)
C       FLDX    FIELD OF INDEPENDENT VARIABLE
C       FLDY    FIELD OF DEPENDENT VARIABLE
C       N       NUMBER OF DATA POINTS
C       M       NUMBER OF CURVES
C       LTYPE 1 LINEAR-LINEAR  2 LINEAR-LOG  3 LOG-LINEAR  4 LOG-LOG
C       IPATRN  FIELD OF DASH PATTERNS FOR CURVES
C       LABY    FIELD OF ALPHA CHARACTERS FOR FLDY LABEL
C       LTIT    FIELD OF ALPHA CHARACTERS FOR TITLE
C       NDX     IF 0 FLDX IS ONE DIMENSIONAL IF 1 FLDX IS 2 DIMENSIONAL
C  IHGR=-1 GRID IS HALFAX  =0 GRID IS GRIDL  =1 GRID IS PERIML
```

```
C   ILAB=0 NO LINE LABELS  =1 LINE LABELS A=FLDY(1) B=2 ETC
      DIMENSION FLDX(N,1),FLDY(N,1),IPATRN(1),LABX(1),LABY(1),LTIT(1)
C     DIMENSION FLDX(L,1),FLDY(L,1),IPATRN(1),LABX(1),LABY(1),LTIT(1)
      DIMENSION IREC(42,40),LSYM(26) ,IG(26)
      DATA(LSYM=1HA,1HB,1HC,1HD,1HE,1HF,1HG,1HH,1HI,1HJ,1HK,1HL,1HM,1HN,
     11HO,1HP,1HQ,1HR,1HS,1HT,1HU,1HV,1HW,1HX,1HY,1HZ)
      IHGP=0
      ILAB=1
      NDX=0
C     M=3
      M=1
      NSEARCH=N
C     NSEARCH=N+2
      DO 20 K=1,1680
   20 IREC(K)=0
      XMIN=XMAX=FLDX(1,1)
      YMIN=YMAX=FLDY(1,1)
      DO 1 J=1,M
      DO 1 I=1,NSEARCH
      YMIN=MIN1F(YMIN,FLDY(I,J))
      YMAX=MAX1F(YMAX,FLDY(I,J))
      IF(NDX.EQ.0.AND.J.GT.1) GO TO 1
      XMIN=MIN1F(XMIN,FLDX(I,J))
      XMAX=MAX1F(XMAX,FLDX(I,J))
 1    CONTINUE
      IF(LFRAME.LT.0)CALL FRAME
      IF(LTYPE.EQ.0)GO TO 8
      GO TO(3,4,5,6)LTYPE
    3 CALL LINRD(XMIN,XMAX,XB,XT,MGRX,INRX,IFMTX,NUMX,IXOR)
      CALL LINRD(YMIN,YMAX,YB,YT,MGRY,INRY,IFMTY,NUMY,IYOR)
      GO TO 7
    4 CALL LINRD(XMIN,XMAX,XB,XT,MGRX,INRX,IFMTX,NUMX,IXOR)
      CALL LGRD (YMIN,YMAX,YB,YT,MGRY,INRY,IFMTY,NUMY,IYOR)
      GO TO 7
    5 CALL LGRD (XMIN,XMAX,XB,XT,MGRX,INRX,IFMTX,NUMX,IXOR)
      CALL LINRD(YMIN,YMAX,YB,YT,MGRY,INRY,IFMTY,NUMY,IYOR)
      GO TO 7
    6 CALL LGRD(XMIN,XMAX,XB,XT,MGRX,INRX,IFMTX,NUMX,IXOR)
      CALL LGRD(YMIN,YMAX,YB,YT,MGRY,INRY,IFMTY,NUMY,IYOR)
    7 CALL SET(.15,.94,.15,.90,XB,XT,YB,YT,LTYPE)
      CALL LABMOD(IFMTX,IFMTY,NUMX,NUMY,1,1,0,0,IXOR)
    8 IF(IHGP)9,10,11
    9 CALL HALFAX(MGRX,INRX,MGRY,INRY,XB,YB,1,1)
      GO TO 12
   10 CALL GRIDL(MGRX,INRX,MGRY,INRY)
      GO TO 12
   11 CALL PERIML(MGRX,INRX,MGRY,INRY)
   12 MM=100-IXOR*90
      CALL PWRT(245,MM,LABX,40,2,0)
      MM=121-NUMY*12
      CALL PWRT(MM,220,LABY,40,2,1)
      CALL PWRT(60,965,LTIT,40,3,0)
      JJ=1
      DO 17 J=1,M
      IF(NDX)JJ=J
      IF(IPATRN(J))13,15,15
   13 DO 14 I=1,N
   14 CALL POINT(FLDX(I,JJ),FLDY(I,J))
```

```
      GO TO 17
15    CALL DASHLN(IPATRN(J))
      IF(IPATRN(J).LE.1) CALL DASHLN(1777B)
      CALL FRSTPT(FLDX(I,JJ),FLDY(I,J))
      DO 18 I=1,N
      CALL VECTOR(FLDX(I,JJ),FLDY(I,J))
      CALL MXMY(MX,MY)
      IX=(MX-130)/20
      IY=(MY-130)/20
      IF(IX.LT.1.OR.IX.GT.41.OR.IY.LT.1.OR.IY.GT.42) GO TO 18
      IF(IREC(IX,IY))33,31,32
31    IREC(IX,IY)=J
      GO TO 18
32    IF(IREC(IX,IY).EQ.J) GO TO 18
33    IF(IREC(IX,IY).LT.-100000000)GO TO 18
      IREC(IX,IY)=-(100*XABSF(IREC(IX,IY))+J)
18    CONTINUE
17    CONTINUE
      CALL DASHLN(1777B)
      IF(M.EQ.1) GO TO 81
      IF(ILAB)80,81
80    CONTINUE
      DO 50 K=1,M
      IG(K)=0
      DO 60 I=1,40
      DO 70 J=1,38
      IF(IREC(I,J).EQ.K)65,70
70    CONTINUE
      GO TO 60
65    CALL PSYM(140+20*I,140+20*J,LSYM(K),1,0,1)
      IG(K)=IG(K)+1
      I=I+10
60    CONTINUE
50    CONTINUE
81    CONTINUE
      IF(LFRAME.GT.0)CALL FRAME
      RETURN
      END
      SUBROUTINE LINRD(XMIN,XMAX,XB,XT,MGRX,INRX,IFMT,NUM,IOR)
      TENLOG=.434294481903
      RANGE=XMAX-XMIN
      IF(RANGE.LT.ABSF(XMIN*1.E-8))RANGE=XMIN*.01
      IF(RANGE)10,11,10
11    XB=1.
      XT=1.
      MGRX=1
      INRX=2
      IFMT=6H(F4.1)
      NUM=4
      IOR=0
      RETURN
10    CONTINUE
      ILGRG=TENLOG*LOGF(RANGE)
      IF(RANGE.LE.1.)ILGRG=ILGRG-1
      RONDRG=10.**ILGRG
      RDN  =RANGE/RONDRG
      RDX=1.
      IF(RDN.LE.6.)RDX=.5
```

```
      IF(RDN.LE.2.)RDX=.2
      DIVSIZ=RONDRG*RDX
      J1=XMIN/DIVSIZ
      IF(XMIN.LT.0.)J1=J1-1
      J2=XMAX/DIVSIZ
      IF(XMAX.GT.0.)J2=J2+1
      IF(J2.EQ.J1)J2=J2+1
      XB=J1*DIVSIZ
      XT=J2*DIVSIZ
      MGRX=J2-J1
      INRX=MIN1F(10.*RDX+.1,5.05)
      IF(ILGRG.LE.0)ID=-ILGRG+1
      IF(ILGRG.GT.0)ID=0
      EPS=1.E-7*DIVSIZ
      IF(ABSF(XB).LE.EPS)1,2
    1 XB=0.
      MINL=2
      GO TO 3
    2 MINL=TENLOG*LOGF(ABSF(XB)) +1
      IF(MINL.LT.1) MINL=1
    3 IF(ABSF(XT).LE.EPS)4,5
    4 XT=0.
      MAXL=2
      GO TO 6
    5 MAXL=TENLOG*LOGF(ABSF(XT)) +1
      IF(MAXL.LT.1) MAXL=1
    6 IF(XB.LT.0)MINL=MINL+1
      IF(XT.LT.0.)MAXL=MAXL+1
      NUM=ID+MAXOF(MINL,MAXL)
      IF(ID)NUM=NUM+1
      IF(NUM.GT.10)8,7
    7 ENCODE(7,100,IFMT)NUM,ID
  100 FORMAT(2H(F,I2,1H.,I1,1H))
      GO TO 9
    8 IF(ID.GT.3)ID=3
      NUM=7+ID
      ENCODE(7,101,IFMT)NUM,ID
  101 FORMAT(2H(E,I2,1H.,I1,1H))
    9 ICRT=12*NUM*MGRX
      IOR=0
      IF(ICRT.GT.790)IOR=1
      RETURN
      END
      SUBROUTINE LGRD(XMIN,XMAX,XB,XT,MGRX,INRX,IFMT,NUM,IOR)
      XMIN=XMIN*1.E-1 $ XMAX=XMAX*1.E+1
      TENLOG=.434294481903
      IXB=TENLOG*LOGF(XMIN) +.001
      IXT=TENLOG*LOGE(XMAX) -.001
      IF(XMIN.LT.1.)IXB=IXB-1
      IF(XMAX.GE.1.)IXT=IXT+1
      IF(IXB.EQ.IXT)IXT=IXB+1
      XB=10.**IXB
      XT=10.**IXT
      MGRX=(IXT-IXB)/2+1
      INRX=(IXT-IXB)/12*10
      NUM=8
      IFMT=6H(E8.1)
      ICRT=(IXT-IXB)*96
```

```
      IF(ICRT.GT.790)IOR=1
      RETURN
      END
*RUN
IAVG (LOG) VS THETA  $S  X  =
 THETA (DEGREES)
 AVERAGE INTENSITY     (LOG)
 ICON (LOG)
 ICON VERSUS THETA
      1.50      0.00 1.D0  181      00.E-6
                                0
      1.40      0.00 1.D0  181      00.E-6
      1.60      0.00 1.D0  181      00.E-6
      1.70      0.00 1.D0  181      00.E-6
      1.80      0.00 1.D0  181      00.E-6
      1.90      0.00 1.D0  181      00.E-6
      2.00      0.00 1.D0  181      00.E-6
      2.10      0.00 1.D0  181      00.E-6
      2.20      0.00 1.D0  181      00.E-6
      2.30      0.00 1.D0  181      00.E-6
      2.40      0.00 1.D0  181      00.E-6
      2.50      0.00 1.D0  181      00.E-6
*END
```